

Equilibrium trapping of cold atoms using dipole and radiative forces in an optical trap

Taro Mashimo, Masashi Abe, and Satoshi Tojo*

Department of Physics, Chuo University, Kasuga, Bunkyo-ku, Tokyo 112-8551, Japan

(Dated: February 4, 2019)

We report on highly effective trapping of cold atoms by a new method for a stable single optical trap in the near-optical resonant regime. An optical trap with the near-optical resonance condition consists of not only the dipole but also the radiative forces, while a trap using a far-off resonance dominates only the dipole force. We estimate a near-optical resonant trap for ultracold rubidium atoms in the range between -0.373 and -2.23 THz from the resonance. The time dependence of the trapped atoms indicates some difference of the stable center-of-mass positions in the near-optical resonant trap, and also indicates that the differences are caused by the change of the equilibrium condition of the optical dipole and radiative forces. A stable position depends only on laser detuning due to the change in the radiative force; however, the position is ineffective against the change in the laser intensity, which results in a change in the radiative force.

I. INTRODUCTION

Optical control of particles and materials is one of the powerful techniques for investigating novel phenomena of media for precise observations in highly qualified isolations [1]. Because of the demonstration of the experimental observation using the optical control for atoms [2], optical tweezer techniques are applied to broad research fields [3, 4], dielectric and metal particles [5, 6], and viruses and bacteria [7]. Moreover, these techniques as optomechanical engineering have been used for realizing precise allocation of atoms [8], levitation of nanoparticles to investigate isolated thermal phenomena [9], etc. Nevertheless, these optomechanics have been applied using the dipole forces only. The radiative force is not preferred because its scattering effect induces dephasing of quantum states, degradation of observation precision, and heating due to spontaneous emission with absorption [10].

For fundamental research studies, optical forces have been developed in the research field of cold atoms because sufficient low density allows collision of atoms in the two-body problem so that experiments are in excellent agreement with theoretical predictions. A far-off resonant trap (FORT) has been investigated and applied for research fields involving cold-atom experiments [11]. The FORT, which has large detuning from the resonance with more than tens of THz typically, can hold cold atoms and quantum degenerates in any spin state for investigating collision properties [12] and spinor Bose-Einstein condensates (BECs) without heating and dephasing the quantum states [13], and to change the shapes of the trap potential and spatial controls of the atoms [14, 15]. The applications of the researches in the FORT mainly involve the use of the dipole forces, called as optical *dipole force* trap. Moreover, although the near-optical resonant trap (NORT), which has a small detuning round of several tens of GHz to several THz, has been treated with

experimental difficulties because of heating, scattering, and dephasing beyond their perturbative conditions by the spontaneous emission [16, 17], there is a possibility of using not only the dipole force but also the radiative force as the hybrid force trap.

In this work, we have investigated the hybrid potential, which consists of the dipole and radiative forces used in the NORT regime while detuning in the range of sub THz to several THz from the resonance. We evaluate the equilibrium trap conditions regardless of the radiative effect, and find that our experimental results of the equilibrium positions are in good agreement with the calculations of the threshold detuning under the condition of stable hybrid forces in a single optical trap.

II. THEORY

A. Dipole and radiative forces in the NORT

The trap beam potential using laser light can be written by the Gaussian beam optics [18]. The electric field amplitude of the propagating beam along the z -axis near the Rayleigh region is approximated as

$$E(r, z) = \frac{E_0}{\sqrt{1 + (z/z_0)^2}} \exp\left[-\frac{r^2}{w^2(z)}\right], \quad (1)$$

where $w(z) = w_0 \sqrt{1 + (z/z_0)^2}$ is the radius of the beam, w_0 is the beam waist, $z_0 = \frac{1}{2}kw_0^2$ is the confocal parameter, and E_0 is the amplitude of the electric field at the center of the beam waist of the trap laser beam. The interaction between the atom and the trap laser beam produces the dipole and radiative forces in the atomic cloud in the trap region [19]. If the detuning of the laser from the atomic resonance δ is sufficiently larger than the natural width of the resonance Γ and the saturation parameter is as small as $s = (\mu^2 E^2 / 2\hbar^2) / (\delta^2 + \Gamma^2 / 4) \ll 1$, the optical dipole and radiative forces at the beam axis F_D and F_R are approximated as

$$F_D = -\frac{\mu^2 E_0^2}{4\hbar} \frac{2zz_0^2}{\delta (z^2 + z_0^2)^2} \quad (2)$$

*Electronic address: tojo@phys.chuo-u.ac.jp

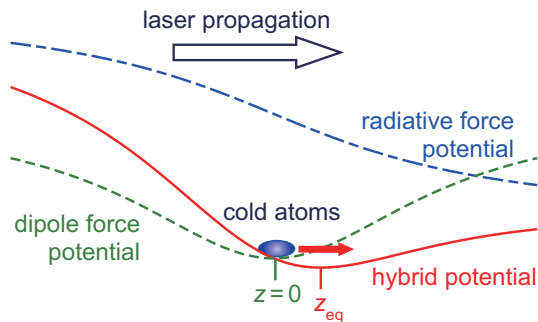


FIG. 1: (color online). Geometry of the cold atoms in the NORT. The trapped atoms located in the focal point have imbalanced effects by the dipole and the radiative forces generating the hybrid potential along with the beam axis of the trap laser.

$$F_R = \frac{\mu^2 k_z \Gamma E_0^2}{4\hbar 2\pi \delta^2} \frac{z_0^2}{z^2 + z_0^2}, \quad (3)$$

where μ is the electric dipole moment of an atom and k_z is the z -component of the wave vector. In the case of the FORT, the radiative force is negligible due to $|\delta| \gg k_z z_0 \Gamma / (4\pi)$ [16]. Therefore, the trap is called an optical *dipole* trap. However, in the case of the NORT, there is a possibility of the existence of an equilibrium condition with variables δ and z due to the presence of the radiative force. As a result, the dipole and radiative forces generate a hybrid trap potential and change the position of the potential minimum. The change in the position due to the hybrid trap forces from that in the optical dipole force is defined as an equilibrium position. The equilibrium position, or the displacement from the initial position, z_{eq} is caused by the balance condition in Eqs.(2) and (3), and is expressed as the solution of the equation $z^2 - 4\pi z |\delta| / (k_z \Gamma) + z_0^2 = 0$ with $-z_0 < z < z_0$ as

$$z_{\text{eq}} = \frac{2\pi|\delta|}{k_z \Gamma} - \sqrt{\left(\frac{2\pi|\delta|}{k_z \Gamma}\right)^2 - z_0^2}. \quad (4)$$

Equation (4) indicates that $|\delta| > k_z^2 w_0^2 \Gamma / (8\pi^2)$ in the presence of equilibrium. Figure 1 illustrates a typical geometry of the trapped cold atoms in the NORT. Owing to the radiative force potential, the total potential of the trap is modified as the hybrid potential from the dipole force potential. The change of the equilibrium position, indicated as z_{eq} , generates variable oscillating motions of the trapped atoms from the initial position $z = 0$. We note that the equilibrium position is independent of the electric field amplitude E_0 .

B. Loading efficiency at a finite temperature in the NORT

Initial loading rate of a typical magneto-optical trap (MOT) to an optical trap depends on the profile of the

trap beam, including the effect of gravity and the temperature of the cold atomic cloud [20]. While loading using an optical beam, the scholar potential generated by the dipole force determines the loading efficiency, and the vector potential generated by the radiative force affects along the beam axis. Owing to the depth of the dipole force potential, the loaded atoms can be trapped on the axis in spite of the existence of the vector potential. The optical dipole force potential in the case of sufficiently small saturation parameter $s \ll 1$ can be expressed as

$$U_D \simeq \frac{\hbar \Gamma^2 I}{8\delta I_s} \quad (5)$$

where I is the laser intensity, and $I_s = 2\pi\hbar c \gamma / 3\lambda^3$ is the saturation intensity. The trap generated by a typical laser beam has a two-dimensional Gaussian profile on the cross section perpendicular to the beam axis. In the electric field of the trap, the trap potential near the Rayleigh region in Eq. (5) can be rewritten as

$$U_D(r, z) = \frac{\epsilon_0 \hbar \Gamma^2 w_0^2 E_0^2}{16 I_s \delta} \frac{1}{w^2(z)} \exp\left[-\frac{2r^2}{w^2(z)}\right] \quad (6)$$

The net trap potential should be modified with an effect of the gravity as $U'_D = U_D(r, z) - u_g(z)$ where $u_g(z)$ is the compensated potential due to the gravity. The modified potential is determined by the profile of the trap beam. In the condition of a typical confinement of the horizontal trap beam for ultracold atoms, $u_g(z)$ can be approximated to be constant as u_{g0} [21].

A thermal atomic cloud is generally loaded into the optical trap up to an energy of 1/10 of the potential depth [20, 21]. We regard the energy as the threshold limit below which the optical trap can hold lower-velocity atoms in accordance with the Maxwell-Boltzmann distribution at a finite temperature. The trapped number of atoms in unit length at z -axis is expressed as the cumulative distribution function of the Maxwell-Boltzmann distribution $h_{\text{MB}}(T, U(r))$ from the atoms with the lowest velocity in the potential $U(r)$ at a temperature of T . By using modified trap potential with an effect of the gravity, we can derive the total number of trapped atoms expressed as

$$N = n_0 \int_{-z_a}^{z_a} \int_0^{r_a} h_{\text{MB}}(T, U'_D(r)) 2\pi r dr dz, \quad (7)$$

where n_0 is the averaged density of the atomic cloud in the trap at a temperature of T , and r_a is the radius of the atomic cloud.

III. EXPERIMENTAL SETUP

A. Cooling setup

The experimental apparatus and procedure used for ultracold ^{87}Rb atoms are almost the same as those described in Ref. [21], except for the optical trap system.

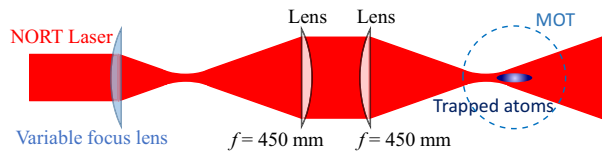


FIG. 2: (color online). Experimental geometry of the NORT. By changing in the focal length of the variable focus lens, the beam parameters of the NORT can be controlled.

We prepare cold ^{87}Rb atoms in a vacuum glass cell using a conventional MOT. After pre-cooling the Rb atoms, we turn off the magnetic-field gradient after the compression and start the polarization gradient cooling (PGC), which consists of two parts. In the first part, the detuning of the cooling laser is swept from -32 to -80 MHz with a decrease of the initial intensity by $1/4$. The second part starts with a frequency jump of the laser locking point from the $F' = 3$ peak to the $F' = 2, 3$ crossover peak. This jump shift of -133 MHz enables large detuning. We use a commercially available laser servo controller (Vescent Photonics Inc., D2-125), which enables the frequency jump with a sample-and-hold circuit. The repump beam detuning is set to -123 MHz to obtain gray-molasses cooling [22, 23]. After the second part, 1.8×10^8 atoms at less than $5 \mu\text{K}$ are typically produced with the cancellation of the residual magnetic field using three Helmholtz coil pairs for highly effective PGC. The coil currents are finely adjusted to minimize the temperature in the molasses after the cooling in the second part. We estimate the residual field to be less than 50 mG. The optical trap beam is switched on after the atom cloud of diameter approximately $400 \mu\text{m}$ is cooled with the cooling and repump beams. The molasses and the optical trap beam are overlapped for 65 ms. In the absence of the overlap, the atoms in the molasses fall off and are separated from the optical trap. The loading of atoms is completed in this period. After loading in the optical trap, the cooling beams and repumping beams are turned off. We change the holding time from 10 to 300 ms to increase the hold time by 10 ms. At the end of holding time, the atoms are irradiated by the weak repumping beam, and almost all the atoms are pumped to the $F = 2$ state. The number of atom and the temperature of the atoms in the optical trap is measured through the absorption imaging after the time of flight.

B. The NORT apparatus

Figure 2 shows the experimental setup of our NORT. The trap beam was generated from a semiconductor laser, and the detuning was adjusted from the D_2 line from -0.37 to -2.23 THz. The collimated trap laser beam passed through the expanding lens system, which consisted of a variable focus lens and two fixed focus

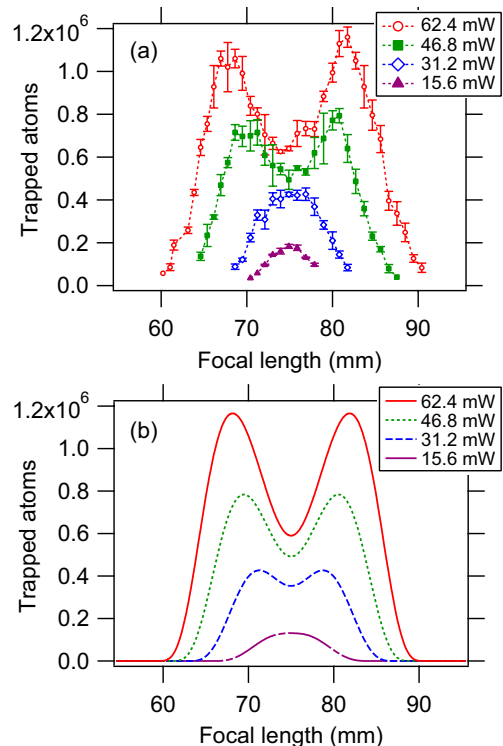


FIG. 3: (color online). Focal length dependence of the number of atoms: (a) Experimental results at 62.4 mW (open circles), 46.8 mW (closed squares), 31.2 mW (open diamonds), and 15.6 mW (closed triangles). (b) Calculations with a single fitting parameter to compensate the number of atoms at 62.4 mW (solid line), 46.8 mW (dotted line), 31.2 mW (dashed line), and 15.6 mW (dotted-dashed line).

lenses with $f = 450$ mm after passing through a single-mode optical fiber to clean up its spatial mode and to improve the spatial stability of the laser beam. The focal length of the variable lens was set at approximately 75 mm to achieve the focus condition at the center of the molasses cloud. The beam profile can be approximated to be a circle, and the focal point can be displaced by changing the focal length of the variable focus lens in the range of $f = 60 - 90$ mm. The beam power was set between 7.8 and 62.4 mW with linear polarization along the horizontal axis. The range of the potential depths was estimated to be from $k_B \times 20$ to $k_B \times 300 \mu\text{K}$. The volume and depth of the trap were dominant for the loading efficiency from the ultracold atomic clouds in the optical molasses condition [21]. By using a tilted 785 -nm band-pass filter, we reduce the scattering and heating effects from the resonance of the D_2 line in the NORT.

IV. RESULTS AND DISCUSSION

We measure the remaining number of atoms in the NORT for 20 ms after loading under changes in the focal

length of the variable focus lens in the range from 60 to 91 mm with $\delta = -1.256$ THz for the detuning of the trap laser and 15.6, 31.2, 46.8, and 62.4 mW of laser power, as shown in Fig. 3 (a). Each point represents a typical average over three samples, with the standard deviation as the error bar. The observed temperatures in the NORT are typically below $10 \mu\text{K}$. The dependence of the number of trapped atoms on the focal length of the variable focus lens shows a symmetricity centered around the focal point in the trap laser beam. When the laser power is high, there are two maximum peaks for the number of trapped atoms, whereas only a single peak is observed for low power values of the laser.

We have numerically calculated the number of trapped atoms using the cumulative distribution function of the Maxwell-Boltzmann distribution for a temperature of $10 \mu\text{K}$ for the atomic clouds, as expressed in Eq. (7). Figure 3 (b) shows the calculation results with one fitting parameter normalized to compensate for the average number of atoms in the two peaks in the experiment with 62.4 mW of the NORT intensity. The trap efficiency is affected by gravity owing to the shallow depth of the potential in the branch side of the optical trap, which reduces the number of trapped atoms in the branch corresponding to a typical difference of $1 \mu\text{K}$. With respect to the potential of the NORT, the radiative force generates the vector potential along the beam axis, whereas the dipole force constructs the scalar potential gathering cold atoms in the initial holding positions. Owing to the characteristics of the vector potential in the NORT, the potential depth in the radial direction remains unchanged, whereas that in the axial direction is modified. The displacement of the atomic cloud is insensitive to the efficiency of atom trapping in the NORT. The calculation results are in good agreement with the experiments, especially when the two maximum peaks can be explained as large trapping volumes that are dominant in the higher power regime. In the case of low power, the calculation results are comparable to those of the experiments for the number of atoms in the trap, although there are some differences for the dependence on focal length. The potential depth of the trap in the low power regime is sensitive to the beam profile of the trap, such as the spatial mode and tilted angle from the horizontal plane of the beam, which reduces the total trap depth generated by the dipole force. The agreements between the calculations and experiments indicate that the dipole force of the NORT determines the efficiency of initial atom trapping, whereas the radiative force has no such effect.

We have measured the time evolution of the trapped atomic cloud in the NORT. The trapped atoms start to move in the trap along the general axial direction. The hybrid trap of the NORT that consists of both the radiative and dipole forces produces an additional radiative force on the atoms as compared to the FORT beam. Figure 4 illustrates the time evolution of the center-of-mass positions of atomic clouds in the NORT for different focal lengths, namely 75.98 mm, 75.50 mm, 75.02 mm, 74.54

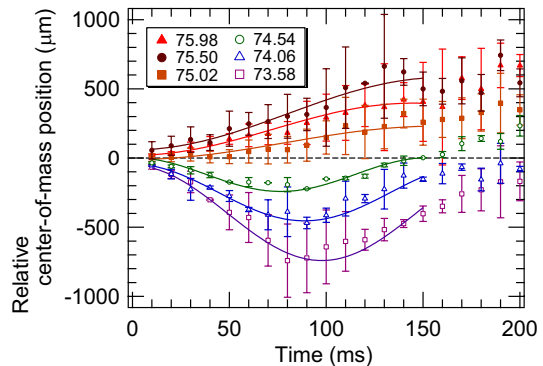


FIG. 4: (color online). Trap time dependence of the center-of-mass positions of the trapped atoms in the NORT. The focal lengths of the variable focus lens are 75.98 mm (closed triangles), 75.50 mm (closed circles), 75.02 mm (closed squares), 74.54 mm (open circles), 74.06 mm (open triangles), and 73.58 mm (open squares). The lines are the fitting curves of the oscillation function obtained from Eq. (8).

mm, 74.06 mm, and 73.58 mm, of the variable focus lens with a detuning of -1.256 THz and trap laser power of 31.2 mW. We define the evolution time of 0 ms to be just after the loading of the NORT with the gray molasses. The initial positions of the atoms are located at the center of the molasses. The zero point of the relative center-of-mass position is defined as the initial position for the focal length of 75.02 mm at the evolution time $t = 0$ ms. The relative center-of-mass positions of the atomic clouds have displacements with oscillation-like behaviors. When the focal lengths exceed 75 mm, the atomic cloud moves to the positive side with the beam propagation. However, when the length is less than 75 mm, the atoms move to negative side. We confirm that there are limitations to the amplitude for the negative region regardless of the fact that there are no limitations in the positive region. Owing to the vector potential of the NORT, the radiative force deforms the trap potential along the beam axis. In the region of the Rayleigh length, the behaviors of atoms initially located at off-focus points can be regarded as a cosine function. Therefore, in Fig. 4, we fit the experimental data with the function

$$z(t) = A \cos(\omega t + \theta) + z_1, \quad (8)$$

where ω is the angular frequency of the oscillation, z_1 is the offset value of the oscillation, and A is the oscillation amplitude of the atomic cloud in the NORT. We consider that the trapped atoms at the initial positions with approximately zero velocity start oscillating in the NORT harmonically with the oscillator potential for $\theta = \pi$.

We have studied the dependence of the amplitudes A from Fig. 4 on the focal length. By linearly fitting the amplitudes A depending on the focal length f , we can find the equilibrium focal length at the zero-crossing point as $A = 0$ and then estimate $f = 75.08$ mm for $\delta = -1.256$ THz. In the case of $A = 0$, the atomic cloud tends to

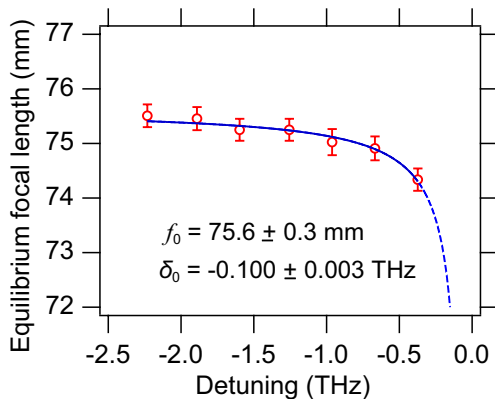


FIG. 5: (color online). Detuning dependence of the equilibrium focal length in balance. The solid curve is fitted using Eq. (4). The dashed line is the extrapolated estimation using the fitting parameters. The fitting results show that the equilibrium focal length $f_0 = 75.6 \pm 0.3$ mm and the threshold of detuning $\delta_0 = -0.100 \pm 0.003$ THz for trapping capability.

stay at the initial position because of the cancellation of the dipole and radiative forces of the NORT in equilibrium condition. The equilibrium focal length is regarded as the most stable position to hold the atoms for a longer trap time. We note that we have fitted the amplitude in the range of more than a few millimeters away from the focus in the initial position and confirmed larger amplitudes with non-harmonic oscillations rather than cosine oscillations.

Figure 5 shows the equilibrium focal length for each frequency of detuning derived from estimation of the non-oscillation focal length with $A = 0$ for each trap time dependence of the center-of-mass positions as those in Fig. 4. For the purpose of compensation for the same trap depth, the laser power values of the NORT are set to 7.8, 17.5, 25.3, 32.5, 43.4, 52.2, and 65.1 mW, corresponding to the frequency detunings $\delta = -0.373, -0.668, -0.962, -1.256, -1.598, -1.891,$ and -2.232 THz, respectively. The equilibrium focal lengths near resonance under $|\delta| < 1.0$ THz suddenly decrease with decrease of the absolute detuning $|\delta|$, whereas those in $|\delta| > 1.0$ THz slightly decrease. We fit the detuning dependence of the equilibrium focal length using Eq. (4) with $z_{\text{eq}} = f_0 - f$, where f_0 is the asymptote focal length. The asymptote to the value of $f_0 = 75.6 \pm 0.3$ mm is close to the focus of the trap beam in the far-off resonant regime. We have confirmed that there is no equilibrium condition in threshold conditions close to the resonance of $\delta \sim -0.15$ THz in our experiments, and the results are comparable to the fitting values of the divergence condition in the detuning case of $\delta_0 = -0.100 \pm 0.003$ THz. The threshold for the divergence is determined by the confocal parameter z_0 and the detuning δ , as expressed by Eq. (4), and it is insensitive to the laser power.

The radiative force in small detunings can generate not only an additional force of the optical trap but also the

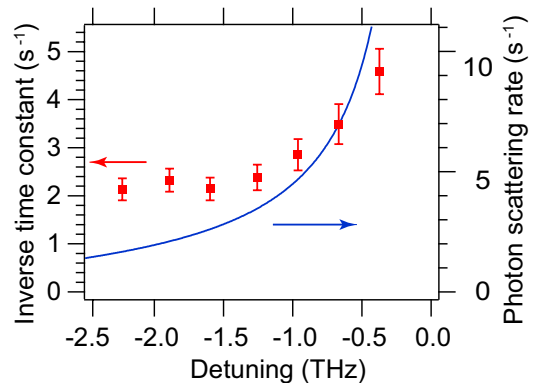


FIG. 6: (color online). Detuning dependence of inversed life-times of trapped atoms in equilibrium conditions, The solid line denotes the photon scattering rates of the NORT on the beam axis.

undesired heating effect caused by the photon scattering. Figure 6 shows the detuning dependence of the inverse time constants of the trapped atoms with the equilibrium focal conditions, and that of the photon scattering rate of the NORT. The experimental results are fitted by the single exponential function owing to one body loss of the trapped atoms in our experimental condition [21]. In the condition of $\delta < 1.0$ THz, the inverse time constant increases owing to the large effect of the radiative force, as shown in Fig. 6. The detuning dependence of the inverse time constants is similar to that of the photon scattering rates. Nevertheless, the quantitative differences in the inverse of time constant in $\delta < 1.0$ THz are only a few factors of magnitude larger than those in $\delta < 1.0$ THz. The results indicate that the NORT in the hybrid trap condition near detuning from sub- to several THz can be applied to ultracold experiments.

The ratio of the equilibrium displacement to the confocal parameter, defined as $R = z_{\text{eq}}/z_0$, informs us of the experimental conditions for realization of the hybrid trap system. In our NORT system, we can estimate the experimental value of $R = 0.030$ with $z_{\text{eq}} = 94 \mu\text{m}$ at $\delta = -2.23$ THz, and $R = 0.40$ with $z_{\text{eq}} = 1.26$ mm at $\delta = -0.373$ THz. The results are comparable to the calculation results: $R = 0.068$ with $z_{\text{eq}} = 215 \mu\text{m}$ at $\delta = -2.23$ THz and $R = 0.51$ with $z_{\text{eq}} = 1.61$ mm at $\delta = -0.373$ THz, respectively. The values of R at the NORT are one or two orders of magnitude larger than those in the FORT for the same optical conditions; *e.g.*, in the system using $\lambda = 1064$ nm, $R = 0.0015$ generates $z_{\text{eq}} = 6.33 \mu\text{m}$ at $\delta = -102$ THz in our trap system. It is roughly estimated that the threshold for the realization of the hybrid trap regime is $R > 0.01$ for the condition where the range of the Rayleigh length in a single trap is a few millimeters. The NORT system has large advantages in comparison with the FORT system because in large detunings the value R is approximately proportional to $1/|\delta|$ and is independent of the laser power. The

sensitivity to the confocal parameter indicates that the radiative force can help the typical off-resonant trap with additional degrees of freedom as the spatial mode, such as the Laguerre-Gaussian mode [24, 25]. In addition, the trap system used in the typical FORT with large R can be realized with a large value of the confocal parameter; *e.g.*, $R > 0.1$ generates $z_{\text{eq}} = 40.1$ mm with $z_0 = 339$ mm in $\delta = -102$ THz with $f = 500$ mm and 1 mm of the beam radius. Regardless of the large $|\delta|$ traps such as the FORT and the general optical tweezer, the hybrid trap can be applied for precise optical control of not only atoms but also nanoscopic and mesoscopic media owing to the effect of the remaining radiative force on the optical trap potential.

V. CONCLUSION

We have achieved a new method of hybrid optical trapping, which consists of both the dipole and radiative forces, using the near optical resonant regime called NORT. We have measured the number of trapped atoms depending on the focal length of the trap and oscillation behaviors in the NORT depending on the detuning of the trap laser with atomic resonance. We have calculated the number of atoms using Gaussian beams with the cumulative function of the Maxwell-Boltzmann dis-

tribution at finite temperature. The calculated results are in good agreement with the experiments and express the larger number of atoms located at off-focus positions. We have estimated the equilibrium position using the hybrid trap and confirmed its power-independent position by comparisons between the experiments and calculations. This hybrid trap has a threshold detuning of $|\delta| > k_z^2 w_0^2 \Gamma / (8\pi^2)$ and is modified to the trap potential with displacements along the beam propagation axis, which is insensitive to the trap laser beam power. The novel optical tweezer system including the radiative force can be applied to precisely control nano- and micro-particles and mesoscopic media in use of multiple traps and higher spatial mode of the trap beams.

Acknowledgments

We would like to thank K. Shibata, S. Takashima, and Y. Iizuka for their assistance in constructing the early experimental setup. This work was supported by the Matsuo Foundation, the Research Foundation for Opto-Science and Technology, Grants-in-Aid for Scientific Research (No. 15K05234) from the Ministry of Education, Culture, Sports, Science, and Technology of Japan, and the Chuo University Joint Research Grant.

-
- [1] D. G. Grier, *Nature* **424**, 810 (2003).
 - [2] S. Chu, J. E. Bjorkholm, A. Ashkin, and A. Cable, *Phys. Rev. Lett.* **57**, 314 (1986).
 - [3] J. D. Miller, R. A. Cline, and D. J. Heinzen, *Phys. Rev. A* **47**, R4567, (1993).
 - [4] T. L. Gustavson, A. P. Chikkatur, A. E. Leanhardt, A. Göllitz, S. Gupta, D. E. Prichard, and W. Ketterle, *Phys. Rev. Lett.* **88**, 020401 (2001).
 - [5] A. Ashkin, J. M. Dziedzic, J. E. Bjorkholm, and S. Chu, *Opt. Lett.* **11**, 288 (1986).
 - [6] K. Svoboda and S. M. Block, *Opt. Lett.* **19**, 930 (1994).
 - [7] A. Ashkin and J. M. Dziedzic, *Science* **235**, 4795 (1987).
 - [8] A. Ashkin, *Proc. Natl. Acad. Sci.* **94**, 4853 (1997).
 - [9] M. Mahamdeh and E. Schäffer, *Opt. Express* **17**, 17190 (2009).
 - [10] H. Metcalf and P. van der Straten, *Laser Cooling and Trapping* (Springer Verlag, New York, USA, 1999).
 - [11] R. Grimm, M. Weidemüller, and Y. B. Ovchinnikov, *Adv. At. Mol. Opt. Phys.* **42**, 95 (2000).
 - [12] S. Tojo, T. Hayashi, T. Tanabe, T. Hirano, Y. Kawaguchi, H. Saito, and M. Ueda, *Phys. Rev. A* **80**, 042704 (2009).
 - [13] D. M. Stamper-Kurn and M. Ueda, *Rev. Mod. Phys.* **85**, 1191 (2013).
 - [14] A. L. Gaunt, T. F. Schmidutz, I. Gotlibovych, R. P. Smith, and Z. Hadzibabic, *Phys. Rev. Lett* **110**, 200406 (2013).
 - [15] J. Leoñard, M. Lee, A. Morales, T. M. Karg, T. Esslinger, and T. Donner, *New J. Phys.* **16**, 093028 (2014).
 - [16] A. Szczepkiewicz, L. Krzemien, A. Wojciechowski, K. Brzozowski, M. Krüger, M. Zawada, M. Witkowski, J. Zachorowski, and W. Gawlik, *Phys. Rev. A* **79**, 013408 (2009).
 - [17] T. Bienaime, S. Bux, E. Lucioni, Ph. W. Courteille, N. Piovella, and R. Kaise, *Phys. Rev. Lett.* **104**, 183602 (2010).
 - [18] L. Mandel and E. Wolf, *Optical coherence and Quantum optics* (Cambridge University Press, New York, USA, 1995).
 - [19] P. D. Lett, W. D. Phillips, S. L. Rolston, C. E. Tanner, R. N. Watts, and C. I. Westbrook, *J. Opt. Soc. Am. B* **6**, 2084 (1989).
 - [20] R. Dumke, M. Johanning, E. Gomez, J. Weinstein, K. Jones, and P. Lett, *New J. Phys.* **8**, 64 (2006).
 - [21] K. Shibata, S. Yonekawa, and S. Tojo, *Phys. Rev. A* **96**, 013402 (2017).
 - [22] A. Hemmerich, M. Weidemüller, T. Esslinger, C. Zimmermann, and T. Hänsch, *Phys. Rev. Lett.* **75**, 35 (1995).
 - [23] D. Boiron, A. Michaud, P. Lemonde, Y. Castin, C. Salomon, S. Weyers, K. Szymaniec, L. Gognet, and A. Clairon, *Phys. Rev. A* **53**, R3734 (1996).
 - [24] V. V. Klimov, D. Bloch, M. Ducloy, and J. R. Rios Leite, *Phys. Rev. A* **85**, 053834 (2012).
 - [25] P. Shumyatsky, G. Milione, and R. R. Alfano, *Opt. Commun.* **321**, 116 (2014).